Optics Communications 291 (2013) 470–475

Contents lists available at SciVerse ScienceDirect

Optics Communications

journal homepage: www.elsevier.com/locate/optcom

High performance spectral-phase surface plasmon resonance biosensors based on single- and double-layer schemes

Cheng Wang [a,b], Ho-Pui Ho [a,*], Ping Shum [c]

[a] Department of Electronic Engineering, Chinese University of Hong Kong, Shatin, NT, Hong Kong SAR, PR China
[b] Department of Microelectronics and Nanoelectronics, Tsinghua University, Beijing 100084, PR China
[c] School of Electrical and Electronic Engineering, Nanyang Technological University, 50 Nanyang Avenue, Singapore 639798, Singapore

ARTICLE INFO

Article history:
Received 27 April 2012
Received in revised form
23 October 2012
Accepted 26 October 2012
Available online 27 November 2012

Keywords:
Surface plasmon resonance
Spectral phase
Biosensors
Wide dynamic range
Multi-layer

ABSTRACT

We have investigated the surface plasmon resonance (SPR) phase change across a range of excitation wavelengths (i.e. spectral-phase) using the Fresnel's equations and Transfer Matrix technique with emphasis on optimizing refractive index sensing performance. Having evaluated the phase change characteristics upon varying different sets of parameters, our results indicate the possibility of achieving extremely high resolution within a wide range of sample refractive index (1.3330–1.3505) at a fixed angle of incidence. We also demonstrate that the double-layer (silver/gold or copper/gold) configuration holds very promising characteristics for SPR sensing, and it is possible to achieve a detection limit of 7.9×10^{-9} RIU (refractive index unit) if one uses a phase measurement resolution of 2×10^{-4} rad. Among all the factors, material of the metal film and its thickness are found to affect performance most. This work provides a comprehensive analysis of the interplay between various system parameters.

1. Introduction

Since the first demonstration of practical biosensors based on surface plasmon resonance (SPR) [1], the SPR sensing technique has seen dramatic advancement in both its technology and application [2]. The basis of SPR is the excitation of highly confined electromagnetic waves, i.e. surface plasmon waves (SPW), which propagate along the dielectric/metal interface. Typical SPR sensors are based on the Kretchmann prism coupling configuration. Efficient excitation is accomplished when the tangential wave vector of the incident p-wave matches with that of the SPW. Coupling conditions follow very sharp resonance characteristics, thus making SPR extremely sensitive to the sample's dielectric constant. This advantage makes SPR a highly promising technology for biological sensing.

SPW coupling occurs in the sample with a certain combination of wavelength and angle of incidence. Reflectivity of the sensing film experiences a dip when we vary the angle of incidence or the excitation wavelength. The reflection coefficients of the p- and s- polarized components (r_p and r_s) are expressed as $r_{p,s}(\lambda)=\sqrt{R_{p,s}(\lambda)}\exp[i\phi_{p,s}(\lambda)]$ [3]. Typical SPR sensors only monitor the change in reflectivity, i.e. $R_{p,s}(\lambda)=|r_{p,s}(\lambda)|^2$, and the corresponding detection limit is around 10^{-5} to 10^{-6} in terms of refractive index unit (RIU) [4,5]. However, excitation of surface plasmon not only comes with a reflectivity dip, but also a dramatic change in differential phase $\Delta\phi(\lambda)=\phi_p(\lambda)-\phi_s(\lambda)$ [6]. In recent years interferometric methods based on phase modulation have been reported to improve detection sensitivity from SPR biosensors by at least 2 orders of magnitude [6–13]. Another advantage of the phase-sensitive SPR approach, as compared to the conventional angular technique, is the convenience to perform SPR biosensing using 2-dimensional sensor arrays. In the angular technique, each sensor site requires a linear array of photodetectors to measure the shift of the SPR dip. This means that an imaging device, which has a 2-dimensional array of photodetectors, can only permit SPR biosensing with a linear array of sensor sites. Although intensity detection at a fixed angle may also achieve 2-dimensional SPR biosensing with an imaging chip, the fact that the reflectivity slopes on both sides of the SPR dip are always less abrupt than that of the phase change leads to the conclusion that the phase-sensitive approach ultimately offers better sensitivity performance than intensity based techniques.

Despite its sensitivity merits, application of phase-sensitive SPR sensor is limited due to its relatively low dynamic range, defined as the refractive index range that sensors can offer best performance. Its dynamic range of 10^{-3} RIU is much smaller than a typical commercial intensity-based sensor (around $\sim10^{-1}$–10^{-2} RIU). Clearly widespread market adoption of the phase-sensitive SPR approach may not happen unless it shows improvement on measurement dynamic range.

* Corresponding author. Tel.: +852 39438279; fax: +852 26035558.
E-mail address: hpho@ee.cuhk.edu.hk (H.-P. Ho).

0030-4018/$ - see front matter © 2012 Elsevier B.V. All rights reserved.
http://dx.doi.org/10.1016/j.optcom.2012.10.064

To resolve the dynamic range issue, phase-sensitive schemes based on the use of white light [14] and the excitation of paired plasmons [15] have been proposed. Indeed the white light phase-sensitive SPR technique, we recently reported, has achieved a detection limit better than 2.6×10^{-7} RIU and a dynamic range of 10^{-2} RIU [16]. Through conducting differential phase measurement across a range of wavelengths, the reported white light interferometric technique has the capability of finding a region of maximum phase transition within the spectrum of the excitation source in order to cover a wide range of sample refractive indices. The performance of SPR sensors is closely associated with a number of system parameters including prism material, choice of material and thickness of metal film, angle of incidence, etc. In addition, although it has been well documented in the literatures that the multi-layer SPR sensor scheme offers promising performance enhancement [6,17,18], there is currently no reported experimental or simulation work on the characteristics of a multi-layer version of the new spectral-phase sensors. Simulation studies on the interplay between various parameters will lead to important insights on the expected performance limits of this new sensor design. Based on the Fresnel's equations and Transfer Matrix technique, one can perform simple but rigorous procedures to optimize the sensor layer structure. Our work focuses on addressing several issues: (1) optimization of sensor parameters for achieving best performance over a relatively wide range of refractive index values (i.e. dynamic range); (2) comparison of the relative performance factors between various metals and their composite layers (e.g. single-layer or double-layer of different materials); and (3) identification of critical parameters that affect sensing performance most.

2. Theory and simulation methods

Since previous literature has shown that the measurement of differential phase using an interferometer is practically feasible and the phase fluctuation is typically 2×10^{-4} rad or 0.01° in most experimental cases of phase-detecting SPR sensors [6,8–11,14,16], we shall use 2×10^{-4} rad as the phase resolution baseline of our simulation. Using this practically achievable phase resolution, we should be able to make fair performance comparison between the proposed scheme and existing SPR biosensing techniques. Additionally, as the findings are based on beam propagation analysis using standard Fresnel's equations, the conclusions should be sufficiently reliable to represent practical situations in general. In the present simulation investigation, the key to performance assessment under different conditions lies in the calculation of differential phase using an appropriate numerical analysis model. Here we use a Transfer Matrix method [3] to cover the single- and double-layer cases.

Fig. 1 shows the transmission and reflection of electromagnetic wave in isotropic multi-layer system. A_k and B_k (k=1, 2,…, n, n is the number of layers, i.e. n=4) are two electromagnetic waves propagating in transmission and in reflection respectively. Using transfer matrix M_{ij} to represent amplitudes in adjacent layers and propagation matrix P_{ij} to represent two interfaces of a particular layer, the n-layer system can be solved by

$$\begin{bmatrix} A_1 \\ B_1 \end{bmatrix} = M_{12}P_2M_{23}P_3\cdots M_{n-1,n}P_n \begin{bmatrix} A_n' \\ B_n' \end{bmatrix} \tag{1}$$

where transfer matrix M_{ij} and propagation matrix P_{ij} are given by

$$M_{ij} = \frac{1}{t_{ij}}\begin{bmatrix} 1 & r_{ij} \\ r_{ij} & 1 \end{bmatrix} \quad \text{and} \quad P_j = \begin{bmatrix} e^{-ik_{yd_j}} & 0 \\ 0 & e^{ik_{yd_j}} \end{bmatrix} \tag{2}$$

where t_{ij} and r_{ij} are p-polarized Fresnel coefficients of transmission and reflection, respectively. These two terms are given by $t_{ij}=2\varepsilon_i k_{yj}/(\varepsilon_i k_{yj}+\varepsilon_j k_{yi})$ and $r_{ij}=(k_{yi}/\varepsilon_i-k_{yj}/\varepsilon_j)/(k_{yi}/\varepsilon_i+k_{yj}/\varepsilon_j)$.

Given the fact that in the n-th layer only downward-propagating EM wave is present, i.e. B_n'=0, the p-polarized reflection coefficient $r_p=B_1/A_1$ can readily be calculated using Eq. (1). By the definition of r_p, the differential phase can be extracted (there is no phase change in s-polarized wave).

In our simulation, we use the first three terms of Sellmeier equation to obtain the refractive index of glass prism [19], i.e. $n^2(\lambda)=1+\sum_{i=1}^{3}B_i\lambda^2/(\lambda^2-C_i)$, where B_i and C_i are constants obtained from Ref. [20]. Dielectric constants of metals are taken from Ref. [21]. Simulation range of incident light wavelength is chosen to match a practical range of sample refractive indices. Also, the sampling resolution is carefully optimized to prevent errors due to aliasing.

For each wavelength in the spectral range under investigation, our program will calculate the differential phase for a range of sample refractive index values. We choose the best detection limit value among all wavelengths for each refractive index data point in order to produce a plot showing the variation of detection limit with respect to RIU value. The phase detection limit is defined as the ratio between phase fluctuation (i.e. 2×10^{-4} rad) and the slope of the differential phase plot.

In our simulation investigation, the refractive index range is fixed at 1.3330–1.3505, which corresponds to that of 0–10 % NaCl in water at room temperature [22] and should be sufficient to cover most biosensing situations. The primary goal is to identify system parameters that will offer best resolution performance.

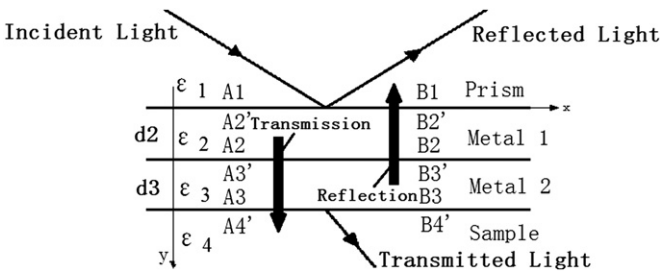

Fig. 1. Schematic diagram of electromagnetic wave propagating in the multi-layer system.

3. Results and discussion

In Fig. 2(a), we show the phase change characteristics versus refractive index for a wavelength range of 680–711 nm. Results are obtained from a typical 51 nm gold/BK7 prism configuration with the angle fixed at 70.9°. Each plot contains a narrow and distinctive region in which a small variation of RIU value will result in very large phase swing. This effectively means that one can always find a suitable spectral peak within the RIU range of interest (i.e. 1.3330–1.3505) for achieving high detection sensitivity. It should be mentioned that the slope of differential phase goes from positive to negative as we change the wavelength across the SPR dip. Indeed, this configuration provides a detection limit better than $10^{-7.19}$ RIU (6.46×10^{-8} RIU) throughout the whole refractive index range of 1.3330–1.3505 (blue line in Fig. 2(b)), which is similar to the experimental data (2.6×10^{-7} RIU) reported in the literature [16]. Fig. 2(b) also shows the variation of detection limit upon changing the angle of incidence. For our wavelength range, varying the angle of incidence only leads to a shift in the refractive index sensing region, while there are marginal changes in the shape of the plots and the absolute

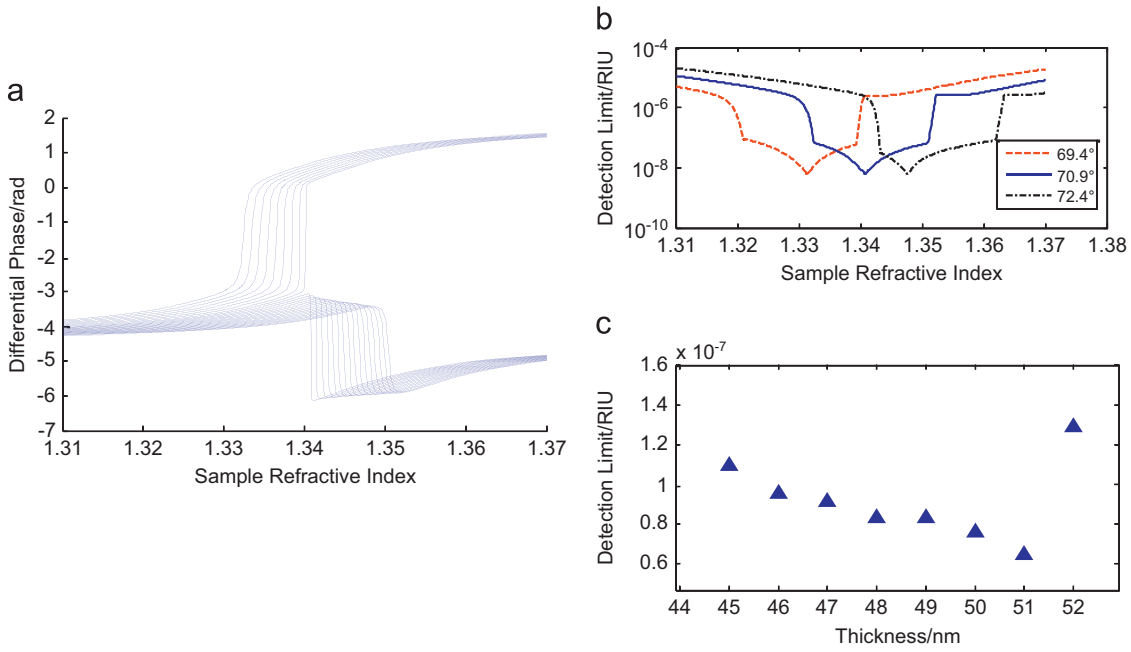

Fig. 2. (a) Differential phase curves for different wavelengths. Systematic conditions: BK7 prism, 51 nm gold film, angle of incidence 70.9°, wavelength range 680–711 nm, wavelength sampling resolution 1.25 nm. (b) System detection limit versus refractive index for different incident angles and (c) Effect of varying gold film thickness. Gold film thickness, angle of incidence and wavelength range for each data point are: 45 nm, 66.1°, 806–1020 nm; 46 nm, 66.5°, 783–943 nm; 47 nm, 67.0°, 760–882 nm; 48 nm, 67.5°, 741–834 nm; 49 nm, 68.3°, 719–787 nm; 50 nm, 69.3°, 700–748 nm; 51 nm, 70.9°, 680–711 nm; and 52 nm, 74.0°, 658–677 nm.

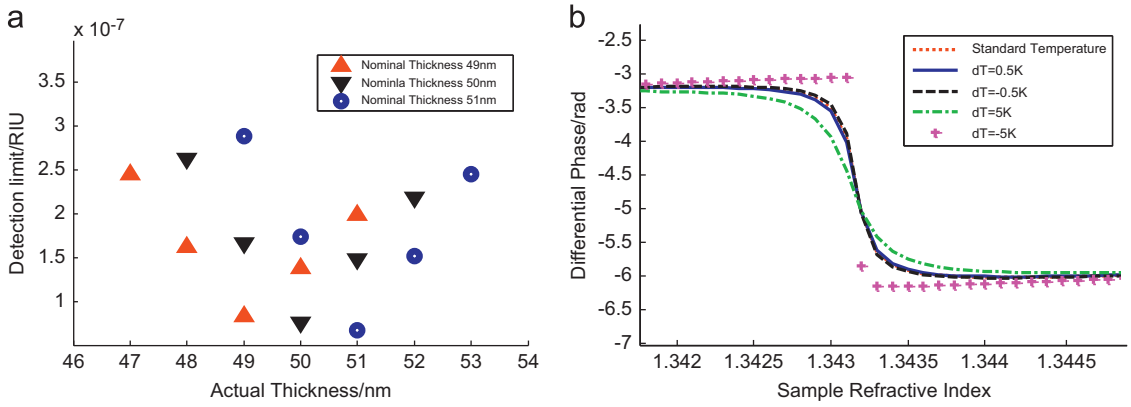

Fig. 3. (a) Effect of errors in controlling the gold film thickness. Systematic conditions for each nominal thickness are set according to Fig. 2(c) and (b) Single-wavelength differential phase curves for different temperature fluctuations.

value of the detection limit, which offers a fast approach to optimize the system when other parameters fixed.

Past research has shown that there exists an optimal thickness under certain conditions for both reflectivity dip and differential phase change [23]. Fig. 2(c) demonstrates the optimized detection sensitivity for a set of thicknesses. Sensitivity improves when metal film thickness increases from 45 nm, and reaches its best at 51 nm. After this peak, detection performance drops rapidly. This means sensing performance degrades less rapidly if the film is thinner than the optimal value. Further investigation shows that this trend is generally true for different metal materials. We have also investigated the effect of metal film uncertainty. Due to run-to-run film deposition variation, thickness uncertainty (± 2 nm) can lead to degradation of SPR sensing performance while the angle of incidence remains fixed to match the nominal thickness (Fig. 3(a)). For each nominal thickness, detection limit degrades to around $10^{-6.80}$ with 1 nm deviation and $10^{-6.60}$ with 2 nm deviation. This indicates that best performance only occurs within a narrow range of thicknesses for a given incident angle. On the other hand, it is interesting to note from Figs. 2(b) and 3(a) that the spectral-phase SPR approach may offer the flexibility of maintaining high detection sensitivity over the RIU range of interest by adjusting the incident angle slightly even when the final sensor film thickness is not exactly identical to the optimum value, e.g. between 49 and 51 nm in the present case.

Another issue is concerned with variation of material constants caused by the deposition process and experimental environment. In a deposition process, the vacuum base pressure, deposition rate and substrate temperature are well under control. To use thickness uniformity, i.e. thickness homogeneity within the sensing area or run-to-run thickness reproducibility, as a main parameter to represent process-related variations in the metal film should be a sensible approach. Here we also simulated for the influence of temperature fluctuations on sensor performance. Using the slope of systematic dielectric constants (metal and glass) versus temperature at different wavelengths [24], the deviations in phase curves are represented in Fig. 3(b) and (c). For ± 0.5 K fluctuation, both the differential phase and detection limit curves almost overlap with the standard

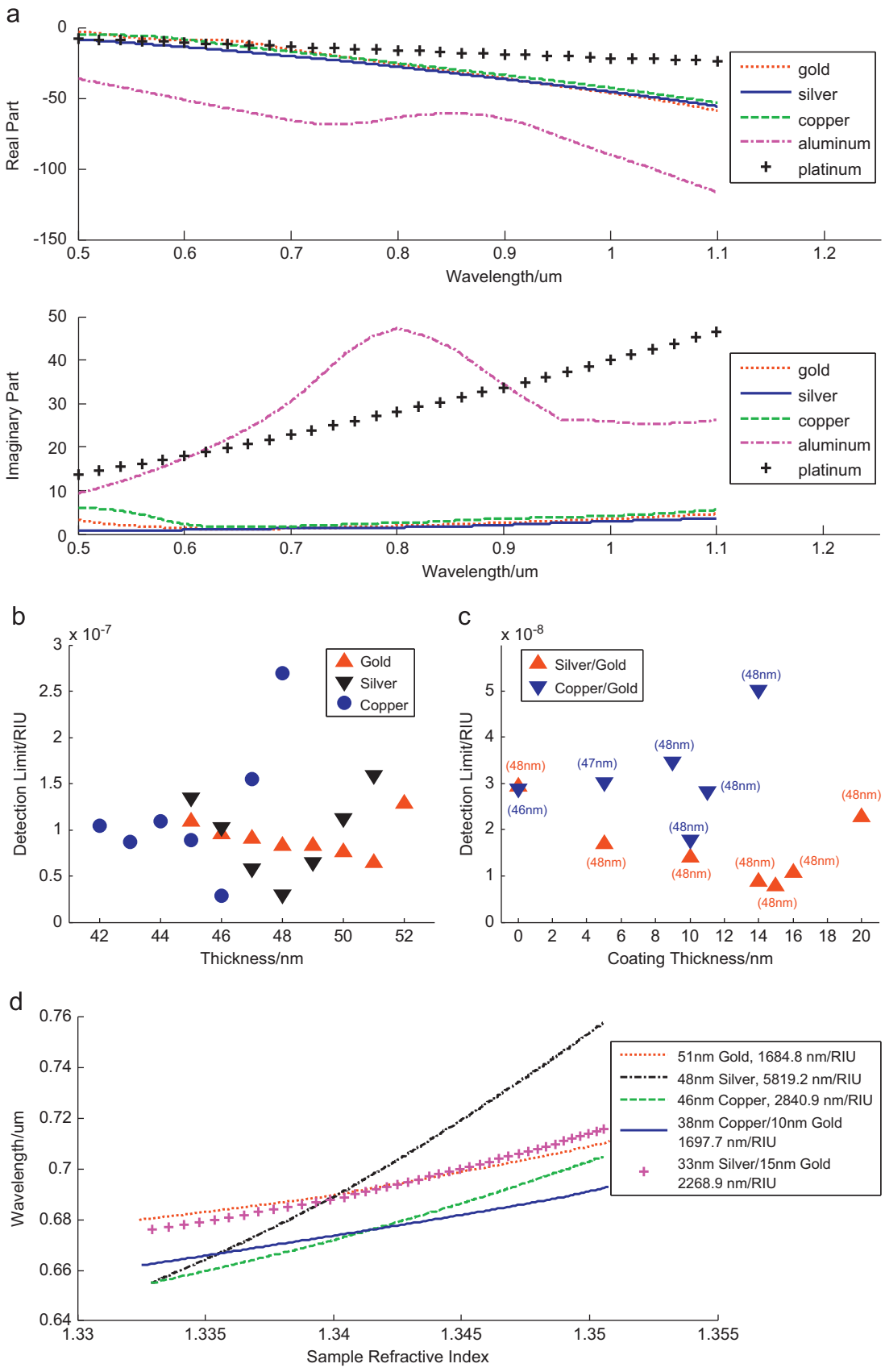

Fig. 4. (a) Dielectric constants of different metals with real and imaginary parts demonstrated respectively. (b) Effect of varying film thickness for single-layer configurations. (c) Effect of varying gold coating thickness for bi-layer configurations. (The number next to the data point indicates the optimal total thickness of sensor film.) (d) Spectral shift range of the SPR dip for optimized single- and double-layer configurations. The inset shows overall resonance wavelength shift per refractive index unit for the whole RI range.

ones, performance degradation is less than 1%. When the temperature fluctuations increase to ± 5 K, the full-range detection limit drops to around $10^{-7.10}$. However, the temperature effect on the sample solution itself turns out to be much more significant. Since the refractive index versus temperature slope of water is around -10^{-4} RIU/K [24], 10^{-4} K temperature resolution is needed to achieve an absolute level of 10^{-8} RIU detection limit. Experimentally one should use an active temperature controller in the sensor head to control the system temperature rigorously.

For many years, gold has been the preferred material for SPR sensors in light of its chemical stability, though silver may offer as much as one order of magnitude improvement in sensitivity limit [7]. We have investigated the dielectric constants of the metals that are known to excite SPR, i.e. gold, silver, copper, aluminum and platinum. Dielectric constants of these metal materials are shown in Fig. 4(a) using data from Ref. [21]. In terms of wavelength dependence, the dielectric constants of gold, silver and copper show similar characteristics. On the other hand, aluminum and platinum exhibit quite different behaviors. In particular, the imaginary part of aluminum and platinum are much larger than those of other materials, thus resulting in rapid optical attenuation inside the medium. The sensor film hence has to be very thin ($\sim$10 nm) in order to excite surface plasmons efficiently. At this thickness, we see neither a sharp reflectivity dip nor any sharp differential phase change. On the other hand, it is interesting to note that there are very few reports on the SPR sensing performance of copper, despite the fact that copper exhibits similar characteristics as gold and silver. We therefore focus our study on the performance comparison between copper and metals of traditional sensing films. Thickness-dependent performance for gold, silver and copper is shown in Fig. 4(b). Our result indicates that the refractive index sensing performance of copper (46 nm, 655–705 nm, 2.88×10^{-8} RIU) is slightly better than silver (48 nm, 655–758 nm, 2.95×10^{-8} RIU), and is significantly better than gold (51 nm, 680–711 nm, 6.46×10^{-8} RIU). Although copper is chemically less inert than silver or gold, its much lower cost may offer a significant advantage, particularly for high volume production of SPR sensor devices.

Until now both silver and copper are not widely adopted in practical sensors because of concerns on layer degradation caused by oxidation. In order to address this issue, it has been reported that a thin gold layer can be used to protect the silver film [6,18]. This composite configuration should provide a reasonable compromise for practical applications. In Fig. 4(c), we show the effect of varying the thickness of the protective gold coating on the performance of the silver/gold and copper/gold composite films. For each gold coating thickness (x-axis), we show the best value of the wide-range detection limit obtained from varying the silver or copper thickness. Indeed very attractive levels of detection limit at 7.94×10^{-9} RIU for 33 nm silver/15 nm gold (70.1° angle of incidence and 676–716 nm wavelength range) and 1.78×10^{-8} RIU for 38 nm copper/10 nm gold (71.6° angle of incidence and 662–693 nm wavelength range) are possible, and this is not achievable by any of the single-layer configurations. These improvements are related to a material matching situation between gold and silver or copper which results in spectral phase characteristics flatter than those associated with the single-layer schemes, thus leading to higher sensing resolution across the whole refractive index range. It is noted that the best-performance data points are largely associated with a common total thickness of 48 nm. Sensing performance primarily depends on the control of the total film thickness, and the system is quite tolerant to thickness variations in individual metal layers. A ± 1 nm deviation in total thickness from the optimal situations will cause the silver/gold and copper/gold system performance to reduce from $10^{-8.10}$ and $10^{-7.75}$ RIU to around $10^{-7.0}$ RIU. In Fig. 4(d), we plot the spectral locations of the SPR dip versus refractive index (1.3330–1.3505) for different cases of double-layer and single-layer configurations.

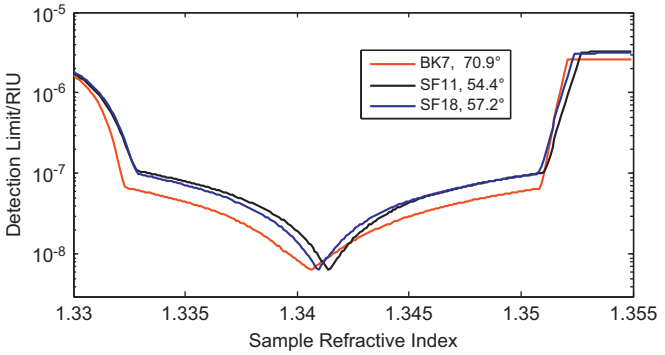

Fig. 5. Effect of varying materials of prism with 51 nm gold film. Angles of incidence and wavelength ranges are: 70.9°, 680–711 nm for BK7; 54.4°, 674–698 nm for SF11; and 57.2°, 676–701 nm for SF18.

We have focused our investigation on detecting the change of bulk refractive index, while in practical situations the sensors have been widely used for studying antigen–antibody interactions (e.g. BSA and BSA antibody) [6,11,12,14,15]. In fact, since SPR is sensitive to local refractive index changes within one wavelength above the sensor surface, such biomolecular interaction events that take place on the surface lead to even higher measurement resolution than that obtained from measuring bulk refractive index changes. In principle, the surface sensitivity increases with bulk sensitivity. However, the relationship between these two may not be linear, since antigen–antibody interactions can also be affected by the surface properties of sensors. We have also calculated the overall shift of the SPR dip per refractive index unit (inset of Fig. 4(d)) for reference. We found that spectral shift range of the single-layer silver case is the highest, approximately double of the other configurations (5819.2 nm/RIU), while the values of other single-layer or double-layer cases are between 1684.8 and 2840.9 nm/RIU.

Other practical factors including surface roughness, wavelength sampling resolution and material of prism also have influence on the sensing performance of spectral-phase SPR. Surface roughness resulting from depositing the metal film under the relatively high pressure can deviate actual SPR curve from simulation, which assumes smooth interfaces. However, Ref. [25] and previous experiments conducted by our team indicate that a surface roughness of RMS around 1 nm does not have much effect on sensing performance. Wavelength sampling resolution is an important parameter since spectral-phase SPR is essentially making use of dispersive effects. Undersampling, particularly near the sharp phase transition region, may lead to degradation of detection sensitivity. In real applications, one may also need to use low-pass filtering for obtaining best-fit information between discrete data points through appropriate interpolation. Until now, BK7 has been chosen in our simulation for the prism. Other high index glass materials, e.g. SF11 and SF18, are also commonly used to permit less oblique angle of incidence. Fig. 5 presents our results on optimized spectral-phase performance using different prism materials. The choice of prism material does not have a significant impact on sensing performance other than a change of incident angle (70.9° for BK7; 54.4° for SF11 and 57.2° for SF18). This finding is primarily due to the fact that these glass materials exhibit similar dispersion trends as described by the Sellmeier equation.

4. Conclusions

We have analyzed the performance of spectral-phase surface plasmon resonance sensor in terms of sensitivity limit and dynamic range using Fresnel's equations and the Transfer Matrix technique. This is the first time that such optimization is being conducted for

the spectral-phase SPR sensor. Our study indicates that extremely high sensitivity of 2.88×10^{-8} RIU across a wide refractive index range (1.3330–1.3505) is achievable with a single layer of copper in the sensing film. The optimized parameters for the copper film thickness, angle of incidence and operation wavelength are respectively 46 nm, 70.5° and 655–705 nm. For silver and gold, the best detection limits are respectively 2.95×10^{-8} RIU (film thickness, angle of incidence and wavelength range are respectively 48 nm, 68.3° and 655–758 nm) and 6.46×10^{-8} RIU (51 nm, 70.9° and 680–711 nm). Above all, the study also reveals that for the double-layer configuration, 7.94×10^{-9} RIU is achievable using a composite film of 33 nm silver/15 nm gold (angle of incidence 70.1°, wavelength range 676–716 nm), and 1.78×10^{-8} RIU is also achievable from a composite film of 38 nm copper/10 nm gold (angle of incidence 71.6°, wavelength range 662–693 nm). This new composite structure is capable of serving the purpose of preventing degradation caused by oxidation of copper or silver. Another advantage of using copper is its much lower material cost in comparison to gold. We have also investigated in detail the effects of different system parameters. It has been found that incident angle, metal film material and thickness are critical parameters for system optimization, while other items including temperature fluctuation, surface roughness, wavelength sampling resolution and material of the prism do not have significant impact on the performance of spectral-phase SPR sensors.

Acknowledgments

The authors wish to acknowledge financial support from a General Research Grant, Hong Kong Research Grants Council, under Project number 412208 and Chinese University of Hong Kong Group Research Project number 3110048.

References

[1] B. Liedberg, C. Nylander, I. Lundström, Sensors and Actuators 4 (1983) 299.
[2] J. Homola, Chemical Reviews 108 (2008) 462.
[3] P.C. Yeh, Optical Waves in Layered Media, Wiley, New York, 1988.
[4] H.P. Ho, S.Y. Wu, M. Yang, A.C. Cheung, Sensors and Actuators B: Chemical 80 (2001) 89.
[5] J. Frischeisen, C. Mayr, N.A. Reinke, S. Nowy, W. Brütting, Optics Express 16 (2008) 18426.
[6] S.Y. Wu, H.P. Ho, W.C. Law, C.L. Lin, S.K. Kong, Optics Letters 29 (2004) 2378.
[7] A.V. Kabashin, P.I. Nikitin, Optics Communications 150 (1998) 5.
[8] C.M. Wu, Z.C. Jian, S.F. Joe, L.B. Chang, Sensors and Actuators B: Chemical 92 (2003) 133.
[9] R. Naraoka, K. Kajikawa, Sensors and Actuators B: Chemical 107 (2005) 952.
[10] Y.D. Su, S.J. Chen, T.L. Yeh, Optics Letters 30 (2005) 1488.
[11] H.P. Ho, W.C. Law, S.Y. Wu, X.H. Liu, S.P. Wong, C.L. Lin, S.K. Kong, Sensors and Actuators B: Chemical 114 (2006) 80.
[12] W. Yuan, H.P. Ho, S.Y. Wu, Y.K. Suen, S.K. Kong, Sensors and Actuators A: Physical 151 (2009) 23.
[13] A.V. Kabashin, S. Patskovsky, A.N. Grigorenko, Optics Express 17 (2009) 21191.
[14] S.P. Ng, C.M.L. Wu, S.Y. Wu, H.P. Ho, S.K. Kong, Biosensors & Bioelectronics 26 (2010) 1593.
[15] C. Chou, H.T. Wu, Y.C. Huang, W.C. Kuo, Y.L. Chen, Optics Express 14 (2006) 4307.
[16] S.P. Ng, C.M.L. Wu, S.Y. Wu, H.P. Ho, Optics Express 19 (2011) 4521.
[17] K. Matsubara, S. Kawata, S. Minami, Optics Letters 15 (1990) 75.
[18] T.T. Ehler, L.J. Noe, Langmuir 11 (1995) 4177.
[19] W. Sellmeier, Annals of Physics 219 (1871) 272.
[20] Optical Glass, Schott Glass Technologies Inc., Duryea, PA, 2010.
[21] E.D. Palik, Handbook of Optical Constants of Solids, Academic Press, Orlando, 1985.
[22] D.R. Lide, CRC Handbook of Chemistry and Physics, 85th ed., CRC Press, Ohio, 2004.
[23] J. Homola, Surface Plasmon Resonance Based Sensors, Springer, Berlin, 2006.
[24] C.S. Moreira, A.M.N. Lima, H. Neff, C. Thirstrup, Sensors and Actuators B: Chemical 134 (2008) 854.
[25] K.M. Byun, S.J. Yoon, D. Kim, S.J. Kim, Journal of the Optical Society of America A 24 (2007) 522.